HEFAT2010
7th International Conference on Heat Transfer, Fluid Mechanics and Thermodynamics
19-21 July 2010
Antalya, Turkey

# STRUCTURAL CHARACTERISTICS OF TURBULENT COMBINED-CONVECTION BOUNDARY LAYERS ALONG A VERTICAL FLAT PLATE

Mohammad Zoynal Abedin [a] and Toshihiro Tsuji [b,*]
*Author for correspondence
a Department of Environmental Technology and Urban Planning, Graduate School of Engineering,
Nagoya Institute of Technology,
Gokiso-cho, Showa-ku, Nagoya 466-8555, Japan,
b Department of Engineering Physics, Electronics and Mechanics, Graduate School of Engineering,
Nagoya Institute of Technology,
Gokiso-cho, Showa-ku, Nagoya 466-8555, Japan,
E-mail: toshihiro.tsuji@nitech.ac.jp

## ABSTRACT

Time-developing direct numerical simulations have been performed for the combined-convection boundary layers induced by imposing aiding and opposing flows to the natural-convection boundary layer in air along a heated vertical flat plate to clarify their structural characteristics. The numerical results show that with a slight increase in freestream velocity, the transition region moves downstream for aiding flow and upstream for opposing flow. This facts correlates well with the existing experimental results showing that the transition delays for aiding flow and quickens for opposing flow in the space-developing boundary layer. Thereby, for aiding flow, turbulence characteristics indicate the behavior proceeding to the laminarization of the boundary layer. On the other hand, for opposing flow, the large scale fluid motions are apparent and become larger than those for the pure natural-convection boundary layer with increasing freestream velocity. For the occurrence of such fluid motions, the budgets of turbulent energy and two-point spatial correlations in the turbulent boundary layer are also examined.

## INTRODUCTION

The turbulent combined-convection boundary layers with various freestreams along a heated vertical flat plate are frequently encountered in many industrial, environmental and engineering fields. In most cases, freestreams are often superimposed on the pure natural-convection boundary layer and the turbulence characteristics vary with the magnitude and direction of freestream and working fluids. However, there are very limited investigations dealing with the fundamental characteristics of the combined-convection boundary layers with aiding and opposing flows along a heated vertical flat plate [1-6]. Some of these researches experimentally revealed that for aiding flow, the heat transfer rates in the combined-convection boundary layer suddenly reduced due to the laminarization of the boundary layer with the increase in freestream velocity [4, 5], while for opposing flow, the heat transfer rates rose with increasing freestream velocity [6]. However, the experiment on these boundary layers is often accompanied by the arrangement of a huge apparatus and the difficulty in obtaining measurements of highly fluctuating velocity and temperature, and thus information obtained from experiments is limited.

To make a breakthrough in such circumstances, we attempted to conduct direct numerical simulations for the time-developing natural-convection boundary layer both in air and water [7] and the combined-convection boundary layers with aiding and opposing flow of air along a heated vertical flat plate [8]. As the results of these simulations, it was revealed that the turbulence statistics for the time-developing boundary layer flows well corresponded with measurements in space-developing flows, when the comparisons were made with the integral thickness of the velocity boundary layer as a characteristic length scale. Therefore, it was confirmed that the practical characteristics of natural- and combined-convection flows could be predicted well with time-developing direct numerical simulations to some extent.

On the other hand, a few experimental investigations were carried out to examine the structural characteristics of the turbulent natural-convection boundary layer [9-12] and the turbulent combined-convection boundary layer with aiding flow of air [5]. However, there are many unclear points for the turbulent structures of these boundary layers, because of a small number of experimental researches.

In the present study, we have investigated the structural characteristics of the turbulent combined-convection boundary layers in air ($Pr$ = 0.71) with various freestreams (adding and opposing flows) along a heated vertical flat plate with a time-

developing direct numerical simulation.

## NOMENCLATURE

| | | |
|---|---|---|
| $g$ | [m/s$^2$] | gravitational acceleration |
| $Gr_x$ | [-] | Grashof number based on $x$ from leading edge of plate in space-developing flow, $g\beta\Delta T_w x^3/\nu^2$ |
| $Gr_\delta$ | [-] | Grashof number based on length scale $\delta$, $g\beta\Delta T_w\delta^3/\nu^2$ |
| $Gr_\lambda$ | [-] | Grashof number based on length scale $\lambda$, $g\beta\Delta T_w\lambda^3/\nu^2$ |
| $h$ | [W/m$^2$K] | heat transfer coefficient |
| $k$ | [W/mK] | thermal conductivity |
| $Nu_x$ | [-] | Nusselt number based on $x$ from leading edge of plate in space-developing flow, $hx/k$ |
| $p$ | [Pa] | pressure |
| $Pr$ | [-] | Prandtl number, $\nu/\alpha$ |
| $Re_\delta$ | [-] | Reynolds number based on length scale $\delta$, $U_\infty\delta/\nu$ |
| $R_{t'}$ | [-] | spatial correlation in the thermal field |
| $R_{u'}$ | [-] | spatial correlation in the streamwise velocity field |
| $T$ | [K] | mean temperature |
| $t$ | [K] | instantaneous temperature |
| $U$ | [m/s] | mean streamwise velocity |
| $u$ | [m/s] | instantaneous streamwise velocity |
| $u_i$ | [m/s] | instantaneous velocity in $x_i$ direction |
| $U_r$ | [m/s] | reference velocity, $(g\beta\Delta T_w\nu)^{1/3}$ |
| $v$ | [m/s] | instantaneous transverse velocity |
| $w$ | [m/s] | instantaneous spanwise velocity |
| $x$ | [m] | vertical distance |
| $x_i$ | [m] | coordinate in tensor notation |
| $y$ | [m] | distance from wall |
| $z$ | [m] | spanwise distance |

Greek symbols

| | | |
|---|---|---|
| $\alpha$ | [m$^2$/s] | thermal diffusivity |
| $\beta$ | [1/K] | coefficient of volume expansion |
| $\Delta T_w$ | [K] | temperature difference between wall and ambient, $T_w$-$T_\infty$ |
| $\delta$ | [m] | integral thickness of the velocity boundary layer |
| $\delta_0$ | [m] | initial value of integral thickness of the velocity boundary layer |
| $\lambda$ | [m] | reference length scale, $2\sqrt{\alpha\tau}$ |
| $\nu$ | [m$^2$/s] | kinematic viscosity |
| $\rho$ | [kg/m$^2$] | density |
| $\tau$ | [s] | time |
| $\omega_x$ | [1/s] | vorticity component in streamwise direction |

Superscripts and Subscripts

| | |
|---|---|
| * | normalized with $\delta_0$ and $\nu$ |
| – | time averaged quantities for experimental statistics and ensemble-averaged quantities for numerical results |
| ' | fluctuating quantities |
| max | maximum value |
| min | minimum value |
| w | wall condition |
| ∞ | ambient condition |

## NUMERICAL PROCEDURE

We consider the time-developing combined-convection boundary layers appended with aiding and opposing freestreams along a heated infinitely long vertical plate at a uniform temperature from a given time onward ($\tau$ = 0). The calculation domain and coordinates are shown in Fig. 1. The coordinates in the vertical, wall-normal and spanwise directions are $x$, $y$ and $z$, respectively, and the instantaneous velocities $u$, $v$ and $w$ are specified in the relevant directions. The wall and ambient temperatures, $T_w$ and $T_\infty$, are assumed to be constant.

The integral thickness $\delta$ of the velocity boundary layer, which is adopted as a characteristic length scale, can be defined as:

$$\delta = \int_0^\infty |U - U_\infty| / (U_{max} - U_{min})\, dy \qquad (1)$$

Here, $U$ is the mean velocity found by averaging the velocity in the ($x$-$z$) plane and $U_\infty$ is the freestream velocity. $U_{max}$ and $U_{min}$ are the maximum and minimum mean velocities in the boundary layer. For natural convection, $U_{min} = U_\infty = 0$ and for combined convection, $U_{min} = 0$ (aiding flow) and $U_{min} = -U_\infty$ (opposing flow).

The boundary layer thickness develops over time from about $4\delta_0$ ($\delta_0$ is the initial value of integral thickness of the velocity boundary layer) in the laminar flow regime to about $40\delta_0$ in the turbulent flow regime. Therefore, the computational domain was set up as $20\pi\delta_0$, $60\delta_0$ and $20\pi\delta_0$ in the $x$, $y$ and $z$ directions, respectively. The governing equations with the Boussinesq approximation expressing the conservation of mass, momentum and energy were numerically solved on a personal computer. The periodic boundary conditions were applied in the $x$ and $z$ directions and the boundary conditions in the y direction were set as: at $y = 0$; $u = v = w = 0$, $t = T_w$ and at $y = 60\delta_0$; $u = v = w = 0$, $t = T_\infty$ for natural convection and $u = \pm U_\infty$, $v = w = 0$, $t = T_\infty$ for combined convection (the sign $\pm$ of $U_\infty$ corresponds to aiding and opposing flows, respectively). The calculations were mainly conducted with (128, 200, 128) grid points in the ($x$, $y$, $z$) directions and the dimensionless time step was set to $2\times10^{-5}$.

The momentum and energy equations were discretized by the second-order-accurate central difference scheme on staggered grids. The calculation of the flow field was advanced with a fractional-step method. The second-order Adams-Bashforth time discretization scheme was adopted to calculate the convective and advective terms and the second-order Crank-Nicholson scheme was used for the viscous, diffusion and buoyancy terms. The nonuniform grids were employed in the $y$ direction and the uniform grids were used in the $x$ and $z$ directions.

The laminar velocity and temperature profiles [8] were given as the initial values at the Grashof number $Gr_{\delta_0} = 3000$ and very small disturbances were added to induce the transition.

## RESULTS AND DISCUSSION

Time-developing direct numerical simulations were conducted by adding various initial disturbances, which have

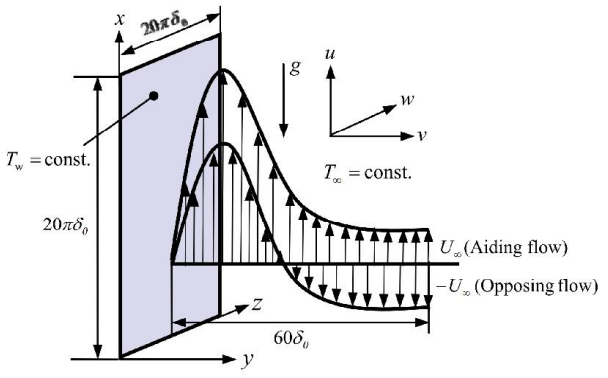


**Figure 1** Calculation domain and coordinates

been created by reducing velocity fluctuations observed in the turbulent boundary layer to tiny fluctuations less than 1 % for the intensities. Such disturbances added in the laminar boundary layer once decay and then become activated showing the commencement of transition. However, these initial disturbances have an effect on the calculated results in the turbulent boundary layer [7]. In fact, the turbulent statistics obtained by averaging instantaneous quantities over the ($x^*$ - $z^*$) planes parallel to the wall vary in some measure with different initial disturbances even for the same Grashof and Reynolds numbers [8]. Therefore, we show the following turbulent statistics as ensemble averaged values of several iterations with different initial disturbances.

**Heat transfer rates and transition behaviour**

The numerical results of the time-developing natural-convection boundary layer are well correlated with measurements in the region from laminar to turbulence of the space-developing boundary layer, when the comparisons are made by employing the integral thickness of the velocity boundary layer $\delta$ as a characteristic length scale [7]. However, the availability of direct numerical simulation for the time-developing boundary layer becomes weak as far as the comparison can be made just with the integral thickness of the velocity boundary layer $\delta$.

Therefore, we examined the relation between the time $\tau$ for the time-developing boundary layer and the distance $x$ from the leading edge of the plate for the space-developing boundary layer. To be concrete, the relation between $\delta$ and the reference length scale $\lambda = 2\sqrt{\alpha\tau}$ for the time-developing natural-convection boundary layer was compared with that between $\delta$ and $x$ for the space-developing natural-convection boundary layer [13]. In consequence, it was found between the Grashof numbers based on $\lambda$ and $x$ that the relation $Gr_x^{1/4} \propto Gr_\lambda$ holds both for the laminar and turbulent boundary layer flows. Thus, we could convert the Grashof number $Gr_\lambda$ for the time-developing natural-convection boundary layer into $Gr_x$ for the space-developing natural-convection boundary layer. For the integral thickness of the velocity boundary layer, numerical data are displayed against the coordinate $Gr_x$ in Fig. 2, comparing with measurements of Tsuji and Nagano [13]. In the figure, $U_r$ is the reference velocity defined as $U_r = (g\beta\Delta T_w \nu)^{1/3}$. Through this process, we could contrast physical quantities for time-developing flow with those for space-developing flow.

The profiles of heat transfer rates in the natural-convection boundary layer and the combined-convection boundary layers both for aiding and opposing flows are shown in Fig. 3 in the relation between the Nusselt number $Nu_x$ and the Grashof number $Gr_x$ based on $x$ from leading edge of plate. It can be seen that, with a slight increase in freestream velocity, the transition region moves downstream for aiding flow and upstream for opposing flow. In other words, for aiding flow, the critical Grashof number $Gr_x$ becomes larger with the increase in aiding freestream velocity and smaller with the increase in opposing freestream velocity. As a result of this transition behaviour varying with the direction and magnitude of freestream, the heat transfer rates in the turbulent combined-convection boundary layers suddenly reduce for aiding flow [2, 4] and further increase for opposing flow [6]. However, the critical Grashof number based on the integral thickness of the velocity boundary layer takes a constant value of about $10^4$ regardless of the direction and magnitude of freestream [8].

**Structural characteristics of turbulent boundary layers**

The contour surfaces of the 3-dimensional vorticity component $\omega_x^*$ ($|\omega_x^*| > 250$) in the $x$ direction are displayed in Fig. 4 for the nearly equivalent Grashof number based on the reference length scale $\lambda$ ($Gr_\lambda$ = $8.4\times10^4$~$8.6\times10^4$). The visualized domain is ($10\pi$, 15, $10\pi$) in the ($x^*$, $y^*$, $z^*$) directions and the positive and negative regions of $\omega_x^*$ are expressed in gray and black, respectively. As seen in Fig. 4(a), the contour surfaces of $\omega_x^*$ observed in the pure natural-convection boundary layer show that large-scale motions meander in the outer region of the boundary layer. However, the contour surfaces of $\omega_x^*$ for aiding flow spread thin as seen in Fig. 4(b).

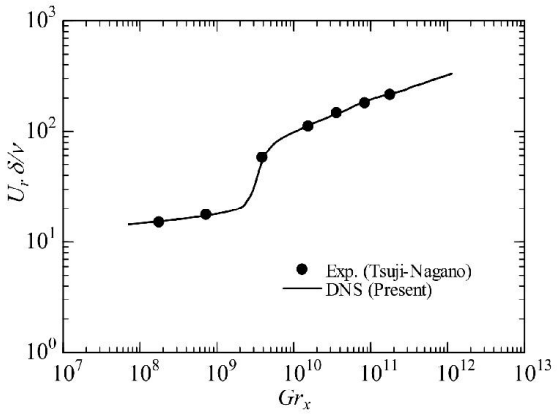


**Figure 2** Variation of integral thickness of the velocity boundary layer

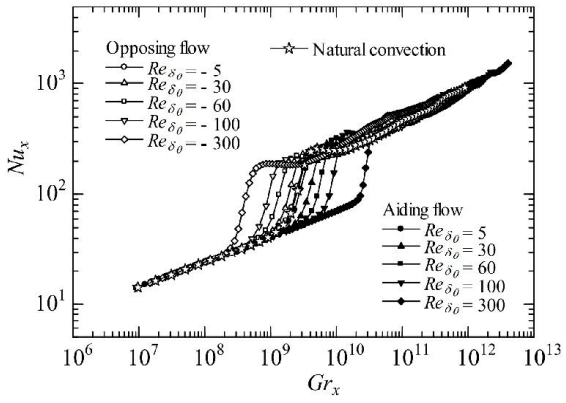


**Figure 3** Relation between Nusselt numbers and Grashof numbers based on $x$

This fact pertains that for combined convection with aiding flow, the long-drawn high- and low-speed regions with weak fluctuations orderly appear in the spanwise direction and the decay of turbulence becomes marked with increasing freestream velocity [8].

On the other hand, the contour surfaces of $\omega_x^*$ for opposing flow as seen in Fig. 4(c) exhibit further complicated and large-scale structures in the whole boundary layer region compared with those for pure natural convection. For reference, the contour surfaces of $\omega_x^*$ for the time-developing forced-convection boundary layer are shown in Fig. 4 (d). It is found that the turbulence structure with streaks of vorticities in the spanwise direction is clearly different from those for the natural- and combined-convection boundary layers.

**Budgets of turbulent energy**

As demonstrated above, the combined-convection boundary layers have unique characteristics in the turbulence structure. Therefore, we examine the turbulent energy transfer process for the velocity field.

By using the Boussinesq approximation, the transport equation of turbulent energy can be written as follows:

$$\frac{D}{D\tau}\left(\frac{1}{2}\overline{q^2}\right)+\frac{1}{\rho}\frac{\partial \overline{pu_k'}}{\partial x_k}+\frac{\partial}{\partial x_k}\left(\frac{1}{2}\overline{q^2u_k'}\right)+\overline{u_i'u_k'}\frac{\partial U_i}{\partial x_k}-g_i\beta\overline{u_i't'}+\varepsilon=0 \qquad (2)$$

(a) (b) (c) (d) (e) (f)

Here, $q^2=u_i'u_i'$ and $\varepsilon=\nu\,\overline{u_i'\partial^2u_i'/\partial x_k^2}$.

In the above equation, (a) - (f) represent advection, pressure diffusion, turbulent diffusion, production, buoyancy production and dissipation, respectively.

The balance of turbulent energy $\overline{q^2}/2$ normalized by $\nu^3/\delta_0^4$ in the turbulent natural-convection boundary layer is shown against $y/\delta$ in Fig. 5. The maximum velocity location corresponds to $y/\delta \approx 0.1$. In the near-wall region, the sum of productions due to buoyancy and deformation of the mean motion is balanced with the sum of turbulent diffusion, pressure diffusion and dissipation, and turbulent energy is transferred to the region very near the wall by viscous diffusion. Also, turbulent energy is transported to the locations near the wall and the maximum velocity by turbulent diffusion. For the balance of turbulent energy in the outer region beyond the maximum velocity location, the calculated values slightly fluctuate from a lack of the number of ensemble average for intermittent fluid motions. Even so, the production due to deformation of the mean motion balances with the sum of turbulent diffusion and dissipation, and turbulent energy is transferred to the maximum velocity location.

Figure 6 shows the balance of turbulent energy in the turbulent combined-convection boundary layer with aiding flow. As seen in the figure, marked production due to deformation of the mean motion is observed in the near-wall region and is balanced with the sum of turbulent diffusion, viscous diffusion and dissipation. Such an appearance of marked production is mainly attributed to the increase in the mean velocity gradient near the wall. However, dissipation of turbulent energy coincidentally increases and fluid motions

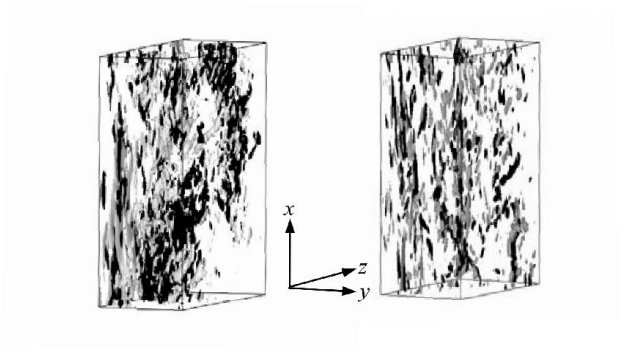


(a) Natural convection: $Gr_\delta = 7.25\times10^6$ $(Gr_\lambda = 8.45\times10^4)$

(b) Combined convection with aiding flow: $Re_\delta = 1.59\times10^3$; $Gr_\delta = 4.51\times10^5$ $(Gr_\lambda = 8.42\times10^4)$

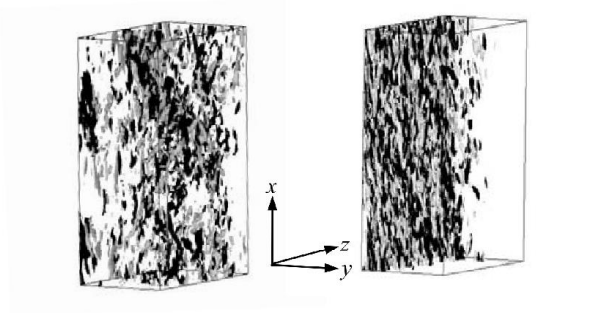


(c) Combined convection with opposing flow: $Re_\delta = -4.64\times10^3$; $Gr_\delta = 1.11\times10^7$ $(Gr_\lambda = 8.6\times10^4)$

(d) Forced convection: $Re_\delta = 5.57\times10^2$

**Figure 4** 3-D contour surfaces of streamwise vorticity: Black; $\omega_x^* < -250$, Gray; $\omega_x^* > 250$

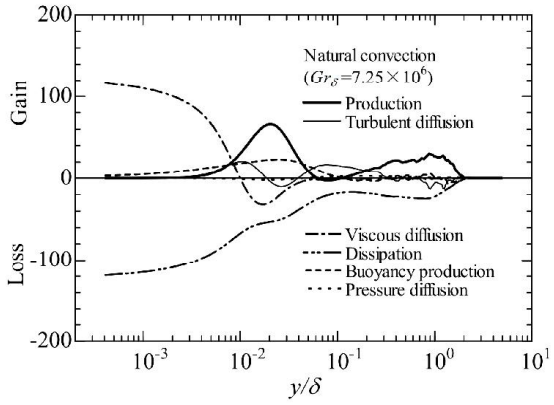


**Figure 5** Balance of turbulent energy in turbulent natural-convection boundary layer

consequently become calm as shown in Fig. 4 (b), which conduces to small buoyancy production. In the outer region of the boundary layer, the balance of turbulent energy is not much different from that in the pure natural-convection boundary layer.

The balance of turbulent energy in the turbulent combined-convection boundary layer for opposing flow is shown in Fig. 7. In the near-wall region, the decrease in the mean velocity gradient leads to a decline in production due to deformation of the mean motion and buoyancy production alternately increases. On the other hand, appreciable production due to deformation of the mean motion appears in the outer region of the boundary layer. It is also observed that turbulent energy produced in the outer region is transported to the near-wall region by turbulent diffusion and dissipation near the maximum velocity location becomes small. Thus, large-scale fluid motions are maintained over the whole boundary layer region as seen in Fig. 4(c).

**Spatial correlations for velocity and thermal fields**

Next, we have examined spatial correlations between two-points in the velocity and thermal fields. A spatial correlation coefficient $R_{u'}(r_y/\delta)$ for streamwise velocity field is defined by the following equation:

$$R_{u'}(r_y/\delta)=\frac{\overline{u'(y/\delta)u'(y/\delta+r_y/\delta)}}{\sqrt{\overline{u'^2(y/\delta)}}\sqrt{\overline{u'^2(y/\delta+r_y/\delta)}}} \tag{3}$$

Here, $y/\delta$ denotes the position of a fixed point in the boundary layer and $r_y/\delta$ is the distance between two points. The two-point spatial correlation coefficients in the thermal field $R_{t'}(r_y/\delta)$ is defined in the same manner. Spatial correlation coefficients predicted for the velocity and thermal fields of the natural-convection boundary layer are plotted in Figs. 8 and 9, respectively, and they are compared with experimental results obtained by Tsuji et al. [10].

As seen in the figures, the predicted profiles correspond relatively well with measurements for approximately equivalent Grashof number. There is an overall similarity between the correlations of velocity and thermal fields. However, a noticeable difference exists in the correlation between the near-wall and outer regions of the velocity and thermal fields (see the

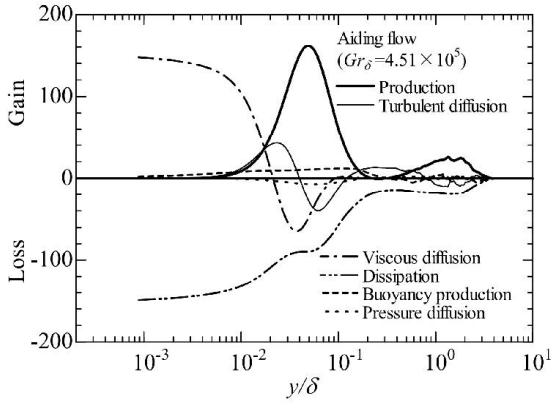


**Figure 6** Balance of turbulent energy in turbulent combined-convection boundary layer with aiding flow

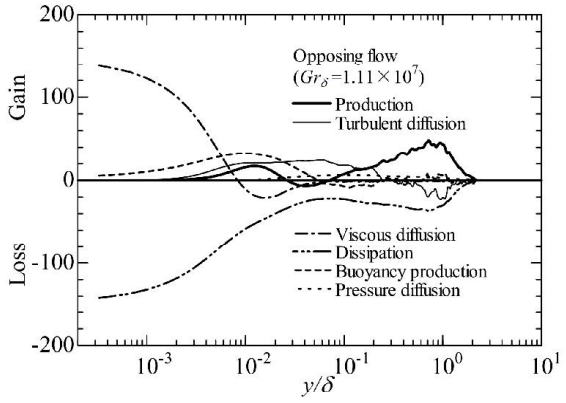


**Figure 7** Balance of turbulent energy in turbulent combined-convection boundary layer with opposing flow

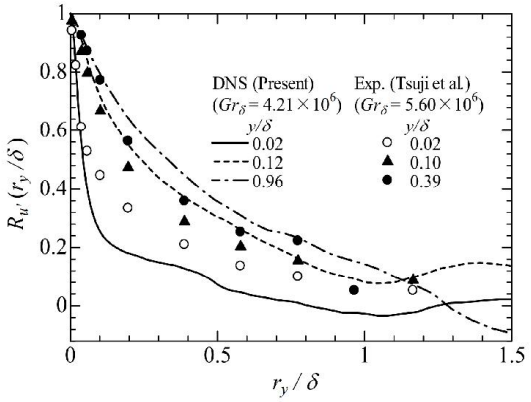


**Figure 8** Spatial correlation for streamwise velocity field for turbulent natural-convection boundary layer

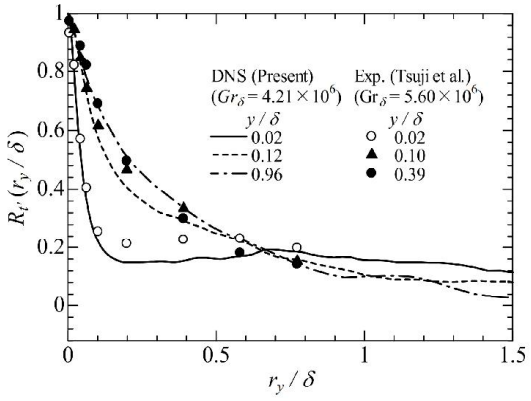


**Figure 9** Spatial correlation for thermal field of turbulent natural-convection boundary layer

results for $y/\delta$ = 0.02). That is, with increasing $r_y/\delta$, the correlation coefficient for the thermal field decreases rapidly in the region up to about the maximum mean velocity location ($y/\delta$ = 0.1) as shown in Fig. 9. Further out, it remains almost constant independent of $r_y/\delta$. As previously reported [14], such constancy in spatial correlation coefficients in the natural-convection boundary layer might be related to one of intermittent bursts and a near-wall structure in the boundary layer might be controlled by this phenomenon. However, as shown in Fig. 8, for the correlation coefficient in the velocity field, no evidence to justify the existence of well-ordered fluid motions similar to those observed in the turbulent forced-convection boundary layer.

The two-point spatial correlation coefficients for the velocity and thermal fields in the combined-convection boundary layers also show approximately equivalent profiles observed in the pure natural-convection boundary layer (not shown in figure).

Although the difference in the spatial correlations between natural- and combined-convection flows cannot be aware of, it is conceived that the turbulent structures of these buoyancy-driven boundary layers are mainly controlled by fluid motions in the outer region of the boundary layer comprehensively judging from the above results.

## CONCLUSION

The structural characteristics of the turbulent combined-convection boundary layers with various freestreams (aiding and opposing flows) in air along a heated vertical flat plate have been numerically investigated with the time-developing direct numerical simulations. The important results obtained are summarized as follows:

(a) With a slight increase in freestream velocity, the transition region moves downstream for aiding flow and upstream for opposing flow. Therefore, heat transfer coefficients for aiding flow rapidly reduce due to the laminarization of the boundary layer with increasing freestream velocity, while those for opposing flow increase with increasing freestream velocity.

(b) For the combined-convection boundary layer with aiding flow, contour surfaces of streamwise vorticity component spread thin, which indicates a process to the laminarization of the boundary layer. In contrast, for opposing flow, contour surfaces of streamwise vorticity component exhibit further complicated and large-scale structures in the whole boundary layer region.

(c) For aiding flow, a marked turbulent energy production due to deformation of the mean motion is observed in the near-wall region, but dissipation of turbulent energy coincidentally increases and fluid motions consequently become calm. On the other hand, for opposing flow, appreciable turbulent energy is produced due to deformation of the mean motion in the outer region of the boundary layer and is transported to the near-wall region by turbulent diffusion.

## ACKNOWLEDGMENTS

The authors would like to acknowledge the Hori Information Science Promotion Foundation, Japan, for the Research Grant (No. 6, 2009-2010) that help partially to carry out the present work.

## REFERENCES

[1] Hall, W. B., and Price, P. H., Mixed forced and natural convection from a vertical heated plate to air, *Proceedings of the 4th International Heat Transfer Conference*, vol. 4, NC 3.3., 1970.

[2] Kitamura, K., and Inagaki, T., Turbulent heat and momentum transfer of combined forced and natural convection along a vertical flat plate - aiding flow, *International Journal of Heat and Mass Transfer*, Vol. 30, No. 1, 1987, pp. 23-41.

[3] Krishnamurthy, R., and Gebhart, B., An experimental study of transition to turbulence in vertical mixed convection flows, *Transactions of the ASME Journal of Heat Transfer*, Vol. 111, 1989, pp. 121-130.

[4] Hattori, Y., Tsuji, T., Nagano, Y., and Tanaka, N., Characteristics of turbulent combined-convection boundary layer along a vertical heated plate, *International Journal of Heat and Fluid Flow*, Vol. 21, No. 5, 2000, pp. 520-525.

[5] Hattori, Y., Tsuji, T., Nagano, Y., and Tanaka, N., Effects of freestream on turbulent combined-convection boundary layer along a vertical heated plate, *International Journal of Heat and Fluid Flow*, Vol. 22, No. 3, 2001, pp. 315-322.

[6] Inagaki, T., and Kitamura, K., Turbulent heat transfer of combined forced and natural convection along a vertical flat plate (Effect of Prandtl number), *Transactions of the JSME B*, Vol. 54, No. 505, 1988, pp. 2515-2522 (in Japanese).

[7] Abedin, M. Z., Tsuji, T., and Hattori, Y., Direct numerical simulation for a time-developing natural-convection boundary layer along a vertical flat plate, *International Journal of Heat and Mass Transfer*, Vol. 52, No. (19-20), 2009, pp. 4525-4534.

[8] Abedin, M. Z., Tsuji, T., and Hattori, Y., Direct numerical simulation for a time-developing combined-convection boundary layer along a vertical flat plate, *International Journal of Heat and Mass Transfer*, Vol. 53, No. (9-10), 2010, pp. 2113-2122.

[9] Tsuji, T. and Nagano, Y., Structural characteristics of a turbulent natural convection boundary layer, *Proceedings of the 2nd China-Japan Work Shop Turbulent Flows*, 1996, pp. 277-289.

[10] Tsuji, T., Nagano, Y., and Tagawa, M., Experiment on spatio-temporal turbulent structures of a natural convection boundary layer, *Transactions of the ASME Journal of Heat Transfer*, Vol. 114, 1992, pp. 901-908.

[11] Kitamura, K., Koike, M., Fukuoka, I., and Saito, T., Large eddy structure and heat transfer of turbulent natural convection along a vertical flat plate, *International Journal of Heat and Mass Transfer*, Vol. 28, No. 4, 1985, pp. 837-850.

[12] Hattori, Y., Tsuji, T., Nagano, Y., and Tanaka, N., Structural characteristics of turbulent natural-convection boundary layer in air along a vertical flat plate heated at high temperature, *Proceedings of the 5th JSME-KSME Fluids Engineering Conference, Nagoya*, 2002, pp. 1-6.

[13] Tsuji, T., and Nagano, Y., Velocity and temperature measurements in a natural convection boundary layer along a vertical flat plate. *Experimental Thermal Fluid Science*, Vol. 2, 1989, pp. 208-215.

[14] Cheesewright, R., and Doan, K. S., Space-time correlation measurements in a turbulent natural convection boundary layer, *International Journal of Heat and Mass Transfer*, Vol. 21 No. 7, 1978, pp. 911-921.